J|A|C|S
ARTICLES
Published on Web 10/02/2002

Structural, Luminescence, and NMR Studies of the Reversible Binding of Acetate, Lactate, Citrate, and Selected Amino Acids to Chiral Diaqua Ytterbium, Gadolinium, and Europium Complexes

Rachel S. Dickins,*,† Silvio Aime,‡ Andrei S. Batsanov,† Andrew Beeby,† Mauro Botta,§ James I. Bruce,† Judith A. K. Howard,† Christine S. Love,† David Parker,*,† Robert D. Peacock,|| and Horst Puschmann†

Contribution from the Department of Chemistry, University of Durham, South Road, Durham, DH1 3LE, U.K., Dipartimento di Chimica IFM, Via P. Giuria, Università degli Studi di Torino, 10125 Torino, Italy, Dipartimento di Scienze e Tecnologie Avanzate, Università del Piemonte Orientale Corso, Borsalino 54, I-10131 Alessandria, Italy, and Department of Chemistry, University of Glasgow, Glasgow, G12 8QQ, U.K

Received June 12, 2002

Abstract: The nature of the ternary complexes formed in aqueous media at ambient pH on reversible binding of acetate, lactate, citrate, and selected amino acids and peptides to chiral diaqua europium, gadolinium, or ytterbium cationic complexes has been examined. Crystal structures of the chelated ytterbium acetate and lactate complexes have been defined in which the carboxylate oxygen occupies an "equatorial" site in the nine-coordinate adduct. The zwitterionic adduct of the citrate anion with [EuL^1] was similar to the chelated lactate structure, with a 5-ring chelate involving the apical 3-hydroxy group and the α-carboxylate. Analysis of Eu and Yb emission CD spectra and lifetimes (H_2O and D_2O) for each ternary complex, in conjunction with ^{1}H NMR analyses of Eu/Yb systems and ^{17}O NMR and relaxometric studies of the Gd analogues, suggests that carbonate, oxalate, and malonate each form a chelated ($q = 0$) square-antiprismatic complex in which the dipolar NMR paramagnetic shift (Yb, Eu) and the emission circular polarization (g_{em} for Eu) are primarily determined by the polarizability of the axial ligand. The ternary complexes with hydrogen phosphate, with fluoride, and with Phe, His, and Ser at pH 6 are suggested to be monoaqua systems with Eu/Gd with an apical bound water molecule. However, for the ternary complexes of simple amino acids with [YbL^1]$^{3+}$, the enhanced charge demand favors a chelate structure with the amine N in an apical position. Crystal structures of the Gly and Ser adducts confirm this. In peptides and proteins (e.g. albumin) containing Glu or Asp residues, the more basic side chain carboxylate may chelate to the Ln ion, displacing both waters.

Introduction

In seeking to devise structural and reactive lanthanide probe complexes for biomolecules,[1,2] two classes may be defined. The first involves systems that are effectively coordinatively saturated in aqueous media, involving octa- or nonadentate ligands that form kinetically stable 1:1 complexes.[3] The interaction with a given biomolecule or ion is likely to be determined primarily by the nature of the ligand, defining complex size, geometry, hydrophilicity, and the relative disposition of hydrogen-bond donors and acceptors. Examples include Eu, Gd, and Tb complexes of enantiopure cationic complexes bearing a pendant phenanthridinium or coordinated tetrazatriphenylene group that have been shown to interact with oligonucleotides and DNA with a selectivity that is a function of base-pair composition and complex helicity.[4,5] Evidence for an intercalative binding mode has also been presented, in certain cases. The second class relates to complexes of heptadentate ligands that are typically diaqua systems of lower overall stability with respect to lanthanide ion dissociation.[2] Here stepwise displacement of the bound water molecules leads to monoaqua and then $q = 0$

* To whom correspondence should be addressed. E-mail: r.s.dickins@dur.ac.uk, david.parker@dur.ac.uk.
† University of Durham.
‡ Università degli Studi di Torino.
§ Università del Piemonte Orientale Corso.
|| University of Glasgow.

(1) Evans, C. H. *Biochemistry of the Lanthanides*; Plenum Press: New York, 1990. *Lanthanide Probes in Life, Chemical and Earth Sciences, Theory and Practice*; Bunzli J.-C. G., Choppin, G. R., Eds.; Elsevier: Amsterdam, 1989.
(2) Dickins, R. S.; Parker, D.; Puschmann, H.; Crossland, C.; Howard, J. A. K. *Chem. Rev.* **2002**, *102*, 1977−2010.
(3) For recent examples, see: Caravan, P.; Ellison, J.; McMurry, T. J.; Lauffer, R. B. *Chem. Rev.* **1999**, *99*, 2293. Platas-Iglesias, C.; Piguet, C.; Andre, N.; Bunzli, J. C. G. *J. Chem. Soc., Dalton Trans.* **2001**, 3084. Andre, N.; Scopelliti, R.; Hopgartner, G.; Piguet, C.; Bunzli, J.-C. G. *Chem. Commun.* **2002**, 214.
(4) Bobba, G.; Frias, J.-C.; Parker, D. *Chem. Commun.* **2002**, 890. Bobba, G.; Kean, S. D.; Parker, D.; Beeby, A.; Baker, G. *J. Chem. Soc., Perkin Trans. 2* **2001**, 1738.
(5) Bobba, G.; Dickins, R. S.; Kean, S. D.; Mathieu, C. E.; Parker, D.; Peacock, R. D.; Siligardi, G.; Smith, M. J.; Williams, J. A. G.; Geraldes, C. F. G. C. *J. Chem. Soc. Perkin Trans. 2* **2001**, 1729. Govenlock, L. J.; Mathieu, C. E.; Maupin, C. L.; Riehl, J. P.; Siligardi, G.; Williams, J. A. G. *Chem. Commun.* **1999**, 1699.

species, the latter being particularly favored with chelating oxyanions. In this regard, the tendency of hydrogen phosphate and fluoride to form monoaqua ternary complexes has recently been contrasted with the ability of hydrogen carbonate to form a chelated carbonate complex in aqueous media.[6]

We hereby report further investigations into the study of the reversible binding of common bioactive oxyanions in aqueous solution to a cationic lanthanide(III) center.[6,7] The emphasis here is on the structural characterization of the ytterbium systems, by crystallographic and solution NMR analysis, with appropriate correlation to their Eu and Gd analogues. The choice of Yb is made for three reasons. First, the high charge density of the cationic Yb complex, $[YbL(OH_2)_2]^{3+}$, enhances the affinity toward oxyanions, with respect to earlier Ln analogues. Second, analysis of the ^{1}H NMR shifts of paramagnetically shifted ligand resonances is relatively simple, being purely dipolar in origin.[8] Moreover, the shift is determined to a considerable extent by the polarizability of the axial donor ligand, allowing information to be gleaned on the nature of the ternary adduct in solution.[9,10] Finally, the chiral Yb complexes are amenable to study by circular dichroism spectroscopy, and the sensitivity of the luminescent $^2F_{5/2}$, excited state of Yb to vibrational quenching by coordinated water molecules has allowed an assessment of complex hydration state to be devised.[11]

Crystal Structures of Ternary Complexes

The diaqua complexes of Eu, Gd, and Yb with the heptadentate ligand (*RRR*)-L^1 were isolated as their trifluoromethanesulfonate salts following reported methods.[6] In the presence of more than a 10-fold excess of added anion, crystals of the ternary complexes of [EuL^1] and [YbL^1] with citrate and acetate, respectively, grew from aqueous solution. For the lactate complexes with [YbL^1] and [HoL^1] and in the case of the glycinate and serinate adducts, 5→10% aqueous methanol was found to be a suitable crystallization solvent. Crystallographic data relating to the lanthanide ion coordination environment are given in Tables 1 and 2,[12] for analyses carried out at 100 or 120 K. Mean bond distances to the macrocyclic ligand N and O donors were in line with those measured[13] for the corresponding nine-coordinate, monoaqua lanthanide complexes of L^2. As the lanthanide ion is permuted, changes in these distances faithfully follow the ionic radius variation,[14] and a common monocapped square antiprismatic coordination geometry is conserved with a twist angle between the N_4 and O_4 planes of ca. 40° in each example (Figure 1). In the case of $[YbL^1OAc]^{2+}$, the C−O distances in the carboxylate were the same [1.267(4) and 1.271(4) Å], consistent with charge delocalization in the bound adduct. The Yb−O distances to the carboxylates differed considerably, being 2.361(2) Å to the oxygen in the equatorial plane and 2.454(2) Å to the axial donor. In the related series of complexes $[YbL^1\text{-lactate}]^{2+}$, $[HoL^1\text{-lactate}]^{2+}$, and [EuL^1-citrate], with a common chelated anion structure (Figure 2), the variation of the bound carboxylate O−Ln distance echoed the ionic radius change. However, the distance of the axial Ln−OH_2 bond remained constant 2.46 (±0.01 Å) (Table 1) and is very similar to the Ln−axial donor distances found for $[YbL^1\text{-OAc}]^{2+}$ (2.454) and $[YbL^2(OH_2)]^{3+}$ (2.440 Å for triflate salt). Given that these axial oxygen donors are likely to have similar

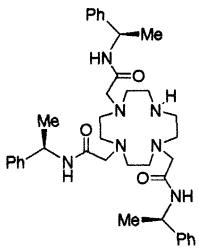

(RRR)- L^1

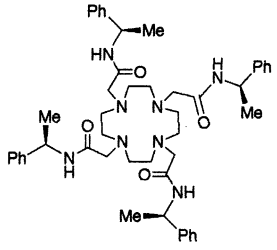

(RRRR) - L^2

Table 1. Bond Distances (Å) for Coordinated Donors in Ternary Complexes with Bound Acetate, Lactate, and Citrate

complex[a]	M–O′$_{axial}$	M–O′$_{eq}$	M–O$_{L^1}$	M–N$_{L^1}$
$[YbL^1OCOMe]^{2+}$	2.454(2)[c]	2.361(2)	2.265(2)	2.530(2)
			2.299(2)	2.549(2)
			2.316(2)	2.585(2)
				2.632(2)
$[YbL^1\text{-lactate}]^{2+}$	2.461(3)[d]	2.278(3)	2.275(3)	2.532(4)
			2.283(3)	2.553(4)
			2.339(3)	2.574(4)
				2.633(4)
$[HoL^1\text{-lactate}]^{2+}$	2.469(3)	2.317(2)	2.308(2)	2.544(3)
			2.313(2)	2.578(3)
			2.359(2)	2.595(3)
				2.653(3)
[EuL^1-citrate]	2.468(2)	2.358(2)	2.332(2)	2.592(3)
			2.378(2)	2.637(3)
			2.393(3)	2.713(3)
				2.722(3)

[a] Counteranion is CF_3SO_3. Acetate at 120 K; lactate structures at 100 K; citrate at 120 K. [b] In the acetate structure the C−O bond distances of the bound carboxylate were 1.267(4) and 1.271(4) Å, while in the Yb and Ho lactate structures, C−O distances of the carboxylate were 1.286(6) and 1.236(7) Å (bound to Yb) and 1.280(5) and 1.247(5) Å (for the Ho example). [c] The axial carboxylate oxygen acts as a hydrogen-bond acceptor to two water molecules that also form H-bonds to a proximate triflate anion. [d] Ionic radii are 1.09 Å (Eu), 1.04 (Ho), and 1.01 (Yb).

Table 2. Bond Distances (Å) for Coordinated Donors in Ternary Complexes with Glycinate and Serinate (120 K)

complex[a]	M–N′$_{ax}$	M–O′$_{eq}$	M–O$_{L^1}$	M–N$_{L^1}$
$[YbL^1\text{-glycinate}]$	2.507(2)	2.264(1)	2.294(1)	2.536(1)
			2.295(1)	2.569(1)
			2.321(1)	2.588(1)
				2.640(1)
$[YbL^1\text{-serinate}]$	2.485(2)	2.271(1)	2.293(1)	2.534(2)
			2.294(1)	2.565(2)
			2.325(1)	2.586(2)
				2.643(2)

[a] $CF_3SO_3^-$ counteranion.

(6) Bruce, J. I.; Dickins, R. S.; Govenlock, L. J.; Gunnlaugsson, T.; Lopinski, S.; Lowe, M. P.; Parker, D.; Peacock, R. D.; Perry, J. J. B.; Aime, S.; Botta, M. *J. Am. Chem. Soc.* **2000**, *122*, 9674.
(7) Kimpe, K.; D'Olieslager, W.; Gorlier-Walrand, C.; Figuerinha, A.; Kovacs, Z.; Geraldes, C. F. G. C. *J. Alloys Compd.* **2001**, *323*, 828.
(8) Bleaney, B. *J. Magn. Reson.* **1972**, *8*, 91. Bertini, I.; Luchinat, C. H. *Coord. Chem. Rev.* **1996**, *150*, 1. Geraldes, C. F. G. C. *NMR in Supramolecular Chemistry*; Pans, M., Ed.; Kluwer: Netherlands, 1999; pp 135−154.
(9) DiBari, L.; Pintacuda, G.; Salvadori, P.; Dickins, R. S.; Parker, D. *J. Am. Chem. Soc.* **2000**, *122*, 9257.
(10) Bruce, J. I.; Parker, D.; Tozer, D. J. *Chem. Commun.* **2001**, 2250.
(11) Beeby, A.; Clarkson, I. M.; Dickins, R. S.; Faulkner, S.; Parker, D.; Royle, L.; de Sousa, A. S.; Williams, J. A. G.; Woods, M. *J. Chem. Soc., Perkin Trans. 2* **1999**, 493.
(12) Details of the Yb and Ho lactate complexes have been described in a preliminary communication: Dickins, R. S.; Love, C. S.; Puschmann, H. *Chem. Commun.* **2001**, 2308.
(13) Dickins, R. S.; Howard, J. A. K.; Maupin, C. L.; Moloney, J. M.; Parker, D.; Riehl, J. P.; Siligardi, G.; Williams, J. A. G. *Chem. Eur. J.* **1999**, *5*, 1095. Aime, S.; Barge, A.; Batsanov, A. S.; Botta, M.; DelliCastelli, D.; Fedeli, F.; Mortillaro, A.; Parker, D.; Puschmann, H. *Chem. Commun.* **2002**, 1120.
(14) Shannon, R. D. *Acta Crystallogr. Ser. C.* **1976**, *32*, 751.

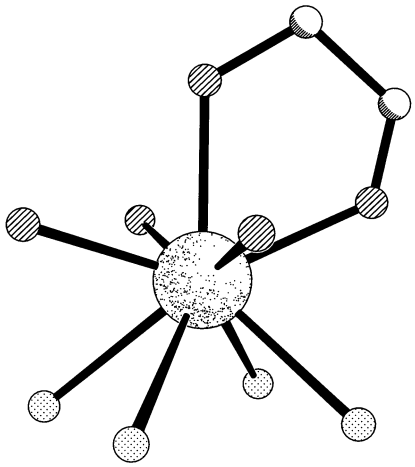

Figure 1. Coordination polyhedron for [EuL[1]-citrate] showing the regular square antiprismatic geometry afforded by the cyclen ring (bottom), the planar array of oxygens (citrate carboxylate plus three ligand amide oxygens), and the axial citrate OH group. Very similar coordination polyhedra were obtained for the chelated complexes with lactate, acetate, and serinate/glycinate).

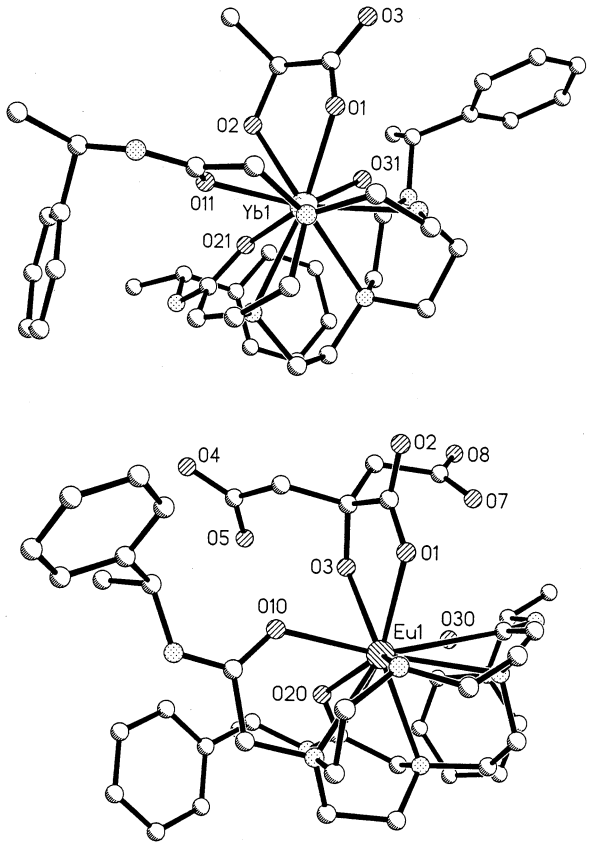

Figure 2. Comparison of the X-ray crystal structures of [YbL[1]-lactate] $(CF_3SO_3)_2$ and [EuL[1]-citrate], showing the common chelate structure.

overall polarizabilities, the uniformity in axial distances suggests that as the smaller Ln ion sits down onto the N_4 plane defined by the macrocyclic ring, a limit is reached due to unfavorable steric interactions or donor atom lone pair repulsion. To examine this hypothesis further, the extent and nature of hydrogen bonding between the axial donor ligand and solvent revealed by the crystallographic study were examined.

In $[YbL^1\ OAc]^{2+}(CF_3SO_3)_2$, (Figure 3), the axial acetate oxygen is hydrogen bonded to two water molecules that, in turn,

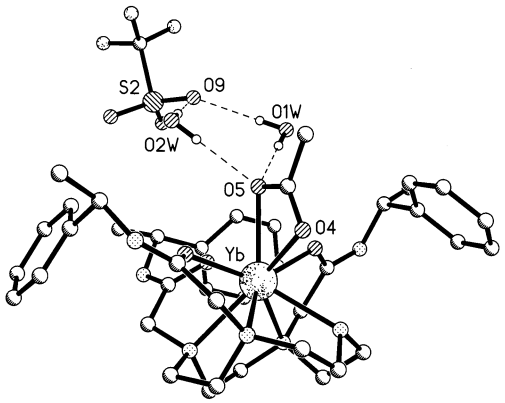

Figure 3. View of the X-ray structure of $[YbL^1OAc](CF_3SO_3)_2(H_2O)_3$ showing the chelated acetate moiety and its hydrogen-bonding interactions to proximate water molecules. Note the absence of any hydrogen-bonding interactions to O(4).

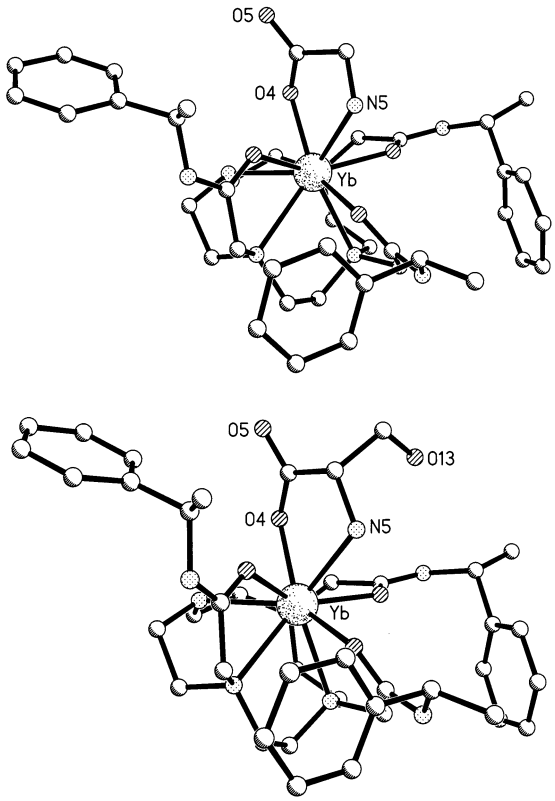

Figure 4. View of the X-ray structure of [YbL[1]-glycinate]$(CF_3SO_3)_2$-$(H_2O)_2$MeOH and of the serinate analogue, showing the common a-amino acid chelate ring with the NH_2 group axially disposed.

form hydrogen bonds to a triflate anion. However, in each of the other structures, the axial OH group (lactate/citrate) or the chelating amino acid NH_2 group was not involved in any hydrogen-bonding interactions to solvent molecules nor to a counteranion. The absence of any significant hydrogen bonding in all but one case supports the hypothesis that the distance between the Ln ion and the axial donor is, to a considerable extent, determined by the minimization of nonbonding repulsive interactions between the macrocyclic ligand and the axial donor.

In the glycinate and serinate ternary complexes (Figure 4), the amino group occupies the axial position and is 2.51 and 2.49 Å distant from the Yb ion. There is a relatively short bond to the carboxylate oxygen (2.26, 2.27 Å) and the other C−O bond forms a hydrogen bond to a proximate MeOH molecule.

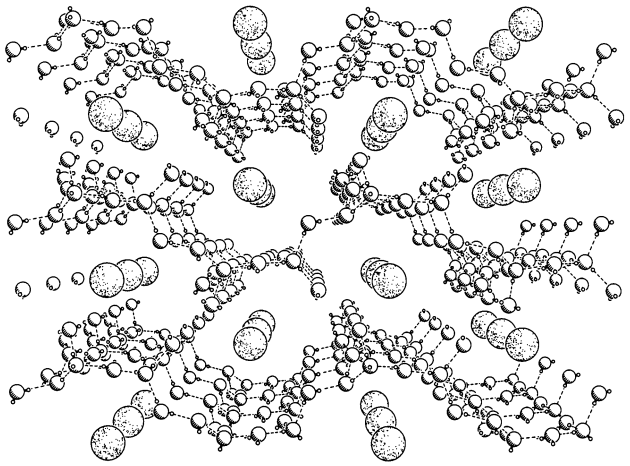

Figure 5. Crystal packing in the structure of [EuL[1]-citrate]$(H_2O)_{11}$ showing the well-defined channels formed by hydrogen-bonded water molecules, filled by the Eu complex moieties.

The amino acid C−O distances in the structures are similar, e.g. 1.280(2) Å to the hydrogen-bonded oxygen and 1.244(4) Å to the Yb-bound oxygen. Such distances may be compared to the mean carbon−oxygen distance in carboxylate anions, which is 1.255(1) Å.[15] There are no previous reports in the CSD of complexes involving α-amino acids and lanthanide ions.

The X-ray analysis of the neutral europium citrate adduct reveals a strongly hydrated structure, with 11 water molecules in the unit cell. This is also the first example of a structurally characterized lanthanide complex involving the citrate anion. A well-defined channel structure was observed, made up of a strongly hydrogen-bonded array of water molecules with the discrete Eu complex moieties running through the channels (Figure 5).

Examples of the structures of lanthanide complexes with glycollate and tartrate have been reported previously,[16,17] of which only one,[18] ($Er(glycollate)_4^-$/$Er(glycollate)_2(H_2O)_4^+$), is not oligomeric in nature. Thus, the lactate structures are also unprecedented in lanthanide structural chemistry, although their formation[1,6]——in common with amino acid chelation[19−22]has been inferred from earlier spectroscopic or pH-metric speciation investigations.

^{1}H NMR, CD, and Emission Spectroscopic Studies of [YbL[1]] Ternary Complexes

Proton NMR spectra in D_2O for $[YbL^1](CF_3SO_3)_3$ were recorded in the presence of an excess (typically > 10 equiv) of a series of oxyanions. Spectra were recorded at 200 MHz (295 K) and exhibited little variation in chemical shift with changes in pD over the range p6 < pD < 8, although amino acid spectra were exchange-broadened at the lower pD (vide infra). Partial ^{1}H NMR spectra, showing the high-frequency region, are presented (Figures 6 and 7) to illustrate the sensitivity of the overall paramagnetic shift to the nature of the added anion. In this region, the most shifted "axial" ring proton is usually observed in complexes possessing a square-antiprismatic coordination environment.[9,23,24] Spectral assignments were made by comparison with related[9] complexes in D_2O, e.g. $[YbL^2]^{3+}$, and by partial ^{1}H−^{1}H COSY analyses. A characteristic feature distinguishing the H_{ax} protons in, say, $[YbL^1OAc]^{2+}$ and $[YbL^1(CO_3)]^+$ (Figures 6 and 7) is that they appear slightly broader

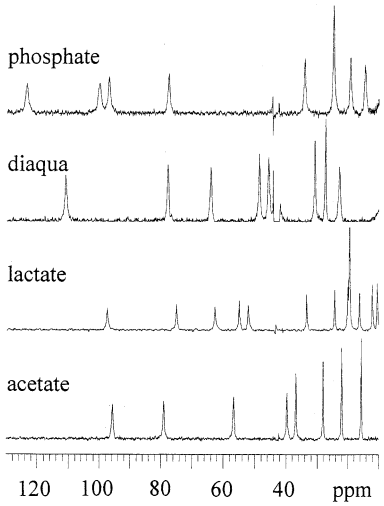

Figure 6. Partial ^{1}H NMR spectra (D_2O, 295 K) for complexes of [YbL[1]] (10 mM) with the following added anions (100 mM): (a) HPO_4^{2-} (pD 7.2); (b) $CF_3SO_3^-$ (pD 6 diaqua species); (c) lactate (pD 6); (d) acetate (pD 6.5). In the lactate complex, the resonances at ca. 55 and 20 ppm are due to the lactate CH and C−Me resonances.

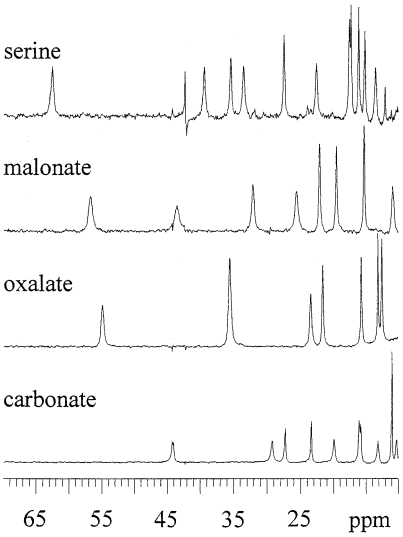

Figure 7. Partial ^{1}H NMR spectra (D_2O, 295 K) for complexes of [YbL[1]] (10 mM) with anions (100 mM) possessing more polarizable donor atoms in the axial site: (a) serinate (pD 6.5); (b) malonate (pD 6); (c) oxalate (pD 6); (d) hydrogen carbonate (pD 7.6). In the spectrum with added serine (a), the resonance at 35 ppm is due to the serinate methine proton.

(15) Allen, F. H.; Kennard, O.; Watson, D. G.; Bramner, L.; Orpen, A. G.; Taylor, R. *International Tables for Crystallography*; 1992, *Vol. C*, Table 9.5.1.1, pp 685−706.
(16) Hawthorne, F. C.; Borys, I.; Ferguson, R. B. *Acta Crystallogr. Sect. C* **1983**, *39*, 540. Trombe, J. C.; Romero, S.; Mosset, A. *Polyhedron* **1998**, *17*, 2529; Grenthe, I. *Acta Chem. Scand.* **1969**, *23*, 1752.
(17) Grenthe, I. *Acta Chem. Scand.* **1972**, *26*, 1479. Grenthe, I. *Acta Chem. Scand.* **1969**, *23*, 1253. Grenthe, I. *Acta Chem. Scand.* **1971**, *25*, 3347. Starynowicz, P.; Meyer, G. *Z. Anorg. Allg. Chem.* **2000**, *626*, 2441.
(18) Grenthe, I. *Acta Chem. Scand.* **1971**, *25*, 3721.
(19) Spaulding, L.; Brittain, H. G. *Inorg. Chem.* **1985**, *24*, 3692. Brittain, H. G. *J. Am. Chem. Soc.* **1980**, *102*, 3693.
(20) Sherry, A. D.; Stark, C. A.; Ascenso, J. R.; Geraldes, C. F. G. C. *J. Chem. Soc., Dalton Trans.* **1981**, 2078. Sherry, A. D.; Pascual, E. *J. Am. Chem. Soc.* **1977**, *99*, 5871. Sherry, A. D.; Yoshida, C.; Birnbaum, E. R.; Darnall, D. W. *J. Am. Chem. Soc.* **1973**, *95*, 3011.
(21) Shelling, J. G.; Bjornson, M. E.; Hodges, R. S.; Taneja, A. K.; Sykes, B. D. *J. Magn. Reson.* **1984**, *57*, 99.
(22) Moeller, T.; Martin, D. F.; Thompson, L. C.; Ferrus, R.; Feistel, G. F.; Randall, W. J. *Chem. Rev.* **1965**, *65*, 1.
(23) Aime, S.; Botta, M.; Ermondi, G. *Inorg. Chem.* **1992**, *31*, 4291. Aime, S.; Botta, M.; Parker, D.; Senanayake, K.; Williams, J. A. G.; Batsanov, A. S.; Howard, J. A. K. *Inorg. Chem.* **1994**, *33*, 4696.
(24) di Bari, L., Pintacuda, G.; Salvadori, P. *J. Am. Chem. Soc.* **2000**, *122*, 5557.

Table 3. Correlation of Ligand Dipolar Proton NMR Shift with the Nature and Polarizability of the Axial Donor in the Ternary Complexes of [YbL[1]] in Aqueous Solution

complex	axial donor	δ_H^{ax}/pmm[a,c]	complex	axial donor	δ_H^{ax}/pmm[a,c]
HPO_4^{2-}	OH_2	100	glycinate	$R'NH_2$	43
F^-	OH_2	99	serinate	$R''NH_2$	43
H_2O	OH_2	75	malonate	$C-O^-$	39
lactate	ROH	71	oxalate	$C-O^-$	37
acetate	$C-\mathbf{O}^{\delta-}$	68	carbonate	$C-O^-$	27

[a] Mean shift of the four 12-N_4 axial ring protons (D_2O, 295 K). [b] Counteranion in each case is a nonligating trifluoromethanesulfonate. [c] A similar general trend is observed in the corresponding Eu complexes, which bind more weakly (especially to OAc^- and the amino acids).[6]

(less sharp) than the shifted H_{eq} ring protons (e.g. for $[YbL^1(CO)_3]^+$, $H_{eq}{}^1$ appears at ca. 27, 23.5, 16.4, and 16.1 ppm). This is a consequence of the larger spin−spin coupling constants for the H_{ax} protons, which experience both a large geminal coupling to H_{eq} and a large vicinal (trans-diaxial) coupling to $H_{ax}{}^1$. Such features have been frequently identified in analyzing related shifted spectra for Yb and Eu complexes involving cyclen-based ligands.[23−25] Values of the mean shift of H_{ax} in each complex are collated in Table 3 and reveal a strong dependence on the nature of the donor atom located in the axial position. The most polarizable donors (e.g. CO_3^{2-} > oxalate > malonate > serinate[26]) give rise to the smallest shift, while the hard uncharged axial donor oxygens in the lactate, aqua, fluoride, and hydrogen phosphate complexes give rise to the largest paramagnetic shift. That fluoride and hydrogen phosphate adducts give the largest shift is also consistent with a reduction in the effective charge at the Yb center in these two cases, reducing the polarizing influence of the Ln ion. A similar trend was observed in the analysis of the NMR spectra of the corresponding $[EuL^1]^{3+}$ adducts, although much higher concentrations of anion needed to be added in order to obtain limiting spectra. This reflects the lower affinity of $[EuL^1]^{3+}$ vs $[YbL^1]^{3+}$ toward anions in water and presumably again relates to the enhanced Lewis acidity and greater polarizing influence of the more charge dense Yb ion. For both, the Eu and Yb ternary adducts, the chemical shift sequence of the ring protons (H_{ax}, H_{eq}), and the diastereotopic exocyclic methylene protons (H_{ac}) followed a common sequence: $H_{ax}{}^1$; $H_{eq}{}^2$, $H_{eq}{}^1$; $H_{ac} \sim H_{ax}{}^2$; $H_{ac}{}'$. Such an order is characteristic of a regular square antiprismatic geometry in each adduct[27]—as revealed by the X-ray structures described herein—and corroborates the premise that axial donor polarizability is the dominant factor in determining the observed magnetic anisotropy.[8−10]

To confirm solution hydration states, the Yb hydration number was estimated using a luminescence method.[11] The rate constant characterizing radiative decay of the $^2F_{5/2}$ Yb excited state was measured for each ternary complex in H_2O and D_2O. Hydration states were estimated using eq 1

$$q^{Yb} = 1.0\,(k_{H_2O} - k_{D_2O} - 0.2) \qquad (1)$$

in which the constant A, with a value of 1.0 μs^{-1}, reflects the sensitivity of the excited Yb ion to vibrational quenching by Yb-bound OH oscillators, and the empirical correction term of 0.2 describes the quenching effect of second sphere waters.[11] The values obtained (Table 4) showed that in the precursor triflate complex $[YbL^1](CF_3SO_3)_3$ there are two bound water molecules, while in the acetate, oxalate, and lactate adduct there are none. For both the fluoride and hydrogen phosphate complexes, one water molecule remained bound, as had been suggested from earlier work with Eu, Gd, and Tb analogues.[6] The axial donor in these two adducts is likely to be a water molecule, as had been implied by analysis of the magnitude of the dipolar shift in ^1H spectra (Table 3). In the case of the amino acid adducts with glycine and serine, values obtained were pH dependent, suggesting a change in structure as the pH was lowered. It is difficult to interpret these data any further, however, as the relative importance of NH quenching on the rate constant for Yb decay has not been defined precisely, yet it is likely to be significant, especially for the chelated structures revealed by the X-ray analysis.

Table 4. Variation of the Rate Constants for Radiative Decay of the Yb $^2F_{5/2}$ Excited State in Ternary Complexes of [YbL[1]] (λ_{ex} 266 nm, 10^{-4} M Complex, 10 mM Anion,[a] pH 7.4, 0.1 M MOPS Buffer)

added anion	k_{H_2O}/ μs^{-1}	k_{D_2O}/ μs^{-1}	q^{Yb} [b]	added anion	k_{H_2O}/ μs^{-1}	k_{D_2O}/ μs^{-1}	q^{Yb} [b]
none (H_2O)	2.50	0.30	2.00	glycinate[c]			
acetate	0.63	0.30	0.13	pH 5	1.11	0.25	0.66
oxalate	0.52	0.22	0.10	pH 10	0.78	0.22	0.36
lactate	0.66	0.17	0.29	serinate[c]			
hydrogen phosphate	1.37	0.35	0.82	pH 5	0.93	0.24	0.49
hydrogen carbonate	0.78	0.24	0.34	pH 10	0.75	0.22	0.33
				fluoride	1.41	0.36	0.85

[a] About 2 mM for glycinate/serinate [b] $q^{Yb} = 1.0$ ($k_{H_2O} - k_{D_2O} - 0.2$). See ref 11 for a discussion; estimated error ±25%. [c] The partial q values here may reflect incomplete complex formation at lower pH and/or the quenching effect of the diastereotopic bound amino acid NH oscillators.

Emission spectra for the $[YbL^1X]$ complexes were measured in D_2O (295 K, 10^{-5} M complex, 10^{-3} M anion), following excitation at 266 nm into the $\pi-\pi^*$ transition of the phenyl absorption band. The series of spectra obtained with $[YbL^1(H_2O)_2]^{3+}$, $[YbL^1X]$ (X = carbonate, oxalate, acetate, malonate), were similar in overall form and intensity. The spectra acquired in the presence of lactate, phosphate, fluoride, and serine were more distinct and afforded a spectral fingerprint. However, the overall complexity of these spectra—arising from the multitude of J sublevels in the $^2F_{7/2}$ and $^2F_{5/2}$ states—precluded any more detailed analysis.[28] Instead, attention was switched to analysis of their near-IR CD spectra examining the region from 920 to 1040 nm. The $^2F_{7/2}-{}^2F_{5/2}$ transitions in Yb^{3+} spectra are globally magnetic-dipole allowed and are among the most sensitive of the Ln series to CD analysis.[29] However, because the separation of the sublevels of the $^2F_{7/2}$ state is less than $1/2kT$ (298 K), the

(25) Aime, S.; Botta, M.; Parker, D.; Williams, J. A. G. *J. Chem. Soc., Dalton Trans.* **1995**, 2259.
(26) In the ^1H NMR of $[YbL^1$-glycinate$]^{2+}$ (D_2O, pD 6, 295 K), a second species (ca. 30% of the major one) was observed at higher frequency that sharpened but did not shift position significantly at pD 9. It may tentatively be assigned to the diastereoisomer of that depicted in the X-ray structure, with a Δ helicity and a ($\lambda\lambda\lambda\lambda$) configuration for the NCCN macrocyclic chelate rings (cf. Figure 1).
(27) For examples of the ^1H NMR analysis of the ring protons in a twisted square antiprismatic geometry that follow a different shift sequence, see: Aime, S.; Barge, A.; Bruce, J. I.; Botta, M.; Howard, J. A. K.; Moloney, J. M.; Parker, D.; de Sousa, A. S.; Woods, M. *J. Am. Chem. Soc.* **1999**, *121*, 5672. Woods, M.; Aime, S.; Botta, M.; Howard, J. A. K.; Moloney, J. M.; Navet, M.; Parker, D.; Port, M.; Rousseaux, O. *J. Am. Chem. Soc.* **2000**, *122*, 9781.
(28) Spectral simplification should be afforded by analysis of circularly polarized emission spectra at variable temperatures:[13] Riehl, J. P.; Richardson, F. S. *Chem. Rev.* **1986**, *86*, 1.
(29) Richardson, F. S. *Inorg. Chem.* **1980**, *19*, 2806.

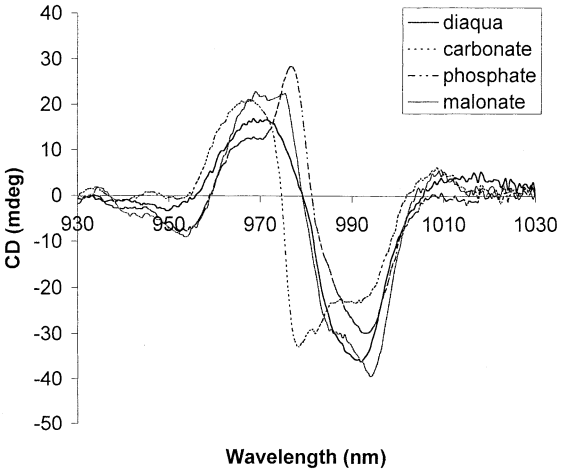

Figure 8. NIR−CD spectra of (*RRR*)-Λ-[YbL^1] as the diaqua, carbonate, hydrogen phosphate, and malonate adducts (295 K, H_2O).

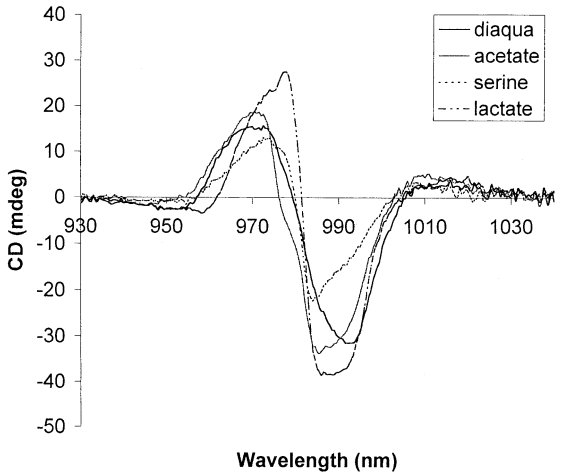

Figure 9. NIR−CD spectra of (*RRR*)-Λ-[YbL^1] as the diaqua, acetate, serine, and lactate adducts (295 K, H_2O).

relative population of these levels is temperature dependent and considerable band overlap occurs. Spectra recorded for (*RRR*)-L-[YbL^{1}X] with differing added anions reveal a clearer pattern than in the corresponding total emission spectra, but further analysis awaits more detailed examination of VT spectra (Figures 8 and 9). The distinctive form of the carbonate and phosphate adducts may be usefully compared: in $[YbL^1(CO_3)]^+$ the positive band at 966 nm is less intense in the hydrogen phosphate adduct, while the bands at 978 nm are apparently of opposite sign. There is more fine structure in the carbonate profile between 980 and 1000 nm, and the positive band at 1010 nm is absent in the phosphate spectrum. Similar spectra were observed with 1-naphthyl analogues of $[YbL^1]^{3+}$, and while the overall form is reminiscent of the CD spectra observed[9] with $[YbL^2X]^{3+}$ (X^1 = H_2O, DMSO, or MeCN), the distinctive changes observed must relate to changes in crystal field splittings that reflect axial donor permutation. Such a conclusion accords with the results obtained in the proton NMR analysis and in the spectral behavior of the corresponding Eu complexes.

Europium and Gadolinium Complexes and the Nature of Amino Acid Complexation

In contrast to Yb emission and CD and CPL spectra, those of Eu complexes are the simplest to interpret and analyze, as a consequence of the absence of degeneracy of the emissive ^5D_o excited state of the Eu^{3+} ion. In earlier work examining reversible oxyanion binding to $[EuL^1]^{3+}$ in water, it was found that Tb ternary complexes were typically an order of magnitude more stable than their Eu analogues. This was considered to reflect both differential complex hydration and the enhanced Lewis acidity of Tb over Eu. The reduced affinity of the Eu adducts means that for the more weakly bound anions, complex formation may only be driven to completion by addition of a very large excess of anion, solubility limits being encountered occasionally. An example is $[EuL^1OAc]^{2+}$, which has an apparent affinity constant of $<10\ M^{-1}$ (295 K, H_2O, pH 7.4)[6] compared to 200 M^{-1} for $[TbL^1OAc]^{2+}$.

Table 5. Variation of Emission Dissymmetry Factors, g_{em}, as a Function of the Bound Anion in Ternary Complexes Based on (*SSS*)-Δ-[EuL^1](CF$_3$SO$_3$)$_3$ (295 K, H_2O, λ_{exc} 255 or 397 nm; 1 mM Complex with >50-fold Excess of Added Anion)

		g_{em}		
		$\Delta J = 1$[a]		$\Delta J = 2$
added anion	likely axial donor	$A_2 \leftarrow A_1$	$E \leftarrow A$	(λ/nm)
none	H_2O	+0.03	**−0.035**	+0.06 (612)
hydrogen phosphate	H_2O	+0.04	**−0.05**	+0.07 (613)
lactate/citrate	R′OH	+0.019	**−0.035**	+0.06 (612)
acetate	$C-O^{1/2-}$	+0.04	**−0.06**	+0.07 (612)
malonate	$C-O^-$	+0.021	**−0.013**	+0.024 (612)
carbonate	$C-O^-$	+0.011	**−0.013**	+0.015 (614)

[a] Typically at 588 and 592 nm respectively, although the splitting of the $A_2 \leftarrow A_1$ and $E \leftarrow A$ components reduces as the axial donor becomes more polarizable, e.g. in the series water > acetate > malonate > carbonate. [b] Values of g_{em} for the ternary complexes of (*R*) or (*S*)-lactate with the racemic complex $[EuL^3]^{3+}$ were also examined (L^3 = achiral analogue of L^1 with benzyl in place of α-MeBn groups) and showed measurable CPL arising from the Pfeiffer effect: (*S*)-lactate giving g_{em} (612 nm) = 0.01 and g_{em} (618) = −0.02 with mirror image spectra for the (*R*)-lactate complex.

Circularly polarized emission spectra for the $[EuL^1]^{3+}$ adducts with HPO_4^{2-}, lactate, citrate, acetate, carbonate, and malonate have been reported earlier.[6] In light of the structural work on the Yb analogues defined herein, the observed dissymmetry factors, g_{em}, for selected transitions may now be correlated with the nature of the likely axial donor in the ternary complex (Table 5). The overall trend, highlighted in analysis of the principal $\Delta J = 2$ transition, is for g_{em} to diminish as the polarizability of the axial donor increases. Thus, the lowest g_{em} values are obtained for the malonate and carbonate complexes, in parallel with the trend seen in analyzing the magnetic anisotropy factor for the Yb analogues (Table 3). A similar pattern has been revealed in the nine-coordinate adducts of the tetramide complex (*SSSS*)-Δ-$[EuL^2]^{3+}$, wherein exchange of the neutral axial donor for more polarizable donors was characterized by a reduction in the $\Delta J = 1$ band splitting, a lowering of the overall ^{1}H NMR paramagnetic shift,[10] and a diminution in the g_{em} values obtained from CPL spectroscopy.[30] Therefore, the change in the circular polarization of the Eu emission following reversible binding of a given anion, e.g. hydrogen carbonate, is primarily a function of the variation in axial donor polarizability and is not due, in this case, to a change in the helicity (twist angle) about the Ln center, as had been provisionally surmised.[6]

Addition of serine (up to 0.15 M) at pD 6.4 to $[EuL^1(H_2O)_2]^{3+}$ (5 mM) was monitored by ^{1}H NMR, and the characteristic spectrum of the diaqua complex (mean H_{ax} at 18.4 ppm, ring

(30) Bruce, J. I.; Lopinski, S.; Parker, D.; Peacock, R. D. *Chirality* **2002**, *14*, 562.

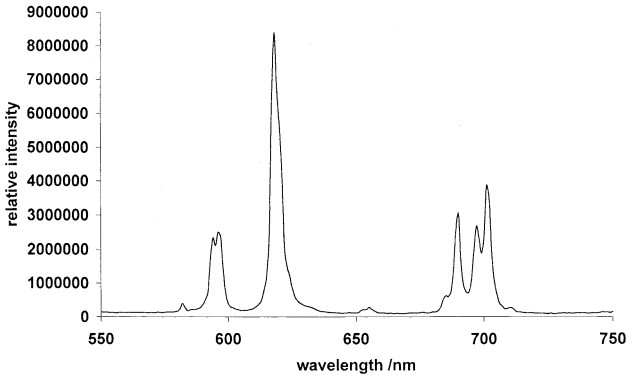

Figure 10. Limiting emission spectrum obtained (H_2O, pH 7.4, 0.1 M MOPS buffer 295 K) following addition of serine to $[EuL^1(H_2O)_2]^{3+}$. A similar spectrum was obtained with added Phe or His.

NH at 11 ppm) was replaced by a rather ill-defined but distinctly different exchange-broadened spectrum (295 K, 200 MHz) that did not sharpen on lowering the temperature to 5 °C. On raising the pH to 10, a new sharper set of signals appeared (mean H_{ax} at 13 ppm) with a reduced overall paramagnetic shift. This solution was examined by emission spectroscopy (295 K, D_2O), and the spectrum obtained revealed a very weak $\Delta J = 0$ transition at 580 nm, a $\Delta J = 1$ manifold in which only two of the expected three components were resolved (2 nm splitting) with a $\Delta J = 2/\Delta J = 1$ intensity ratio of ca. 3:1. The same spectrum was obtained in buffered solution (pH 7.4). The spectrum (Figure 10) was more or less invariant over the pH range 7−10, but below pH 7 it became less well resolved. Almost identical spectra were recorded, under the same conditions, with excess added Phe, Ala, or His. Incremental addition of Phe and His was monitored by examining the change in intensity of the Eu emission band at 618 nm, and nonlinear least squares iterative data fitting gave apparent association constants for the 1:1 adduct of 120(±20) M^{-1} and 3500(±500) M^{-1} for Phe and His respectively (295 K, pH 7.4, 0.1 M MOPS). The higher apparent value for the His adduct may reflect a more favorable free energy of solvation in the complex, due to hydrogen bonding involving the imidazole nitrogens.

The relaxivity of $[GdL^1(H_2O)_2](CF_3SO_3)_3$ in aqueous solution is 8.5 mM^{-1} s^{-1} (20 MHz, 298 K, pH 6.2)[6] and is typical of a $q = 2$ complex with this molecular size.[31] At higher pH values, carbonate (from CO_2 in solution) begins to bind, and beyond pH 9, amide NH deprotonation also occurs, enhancing relaxivity. Measurements of relaxivity versus added amino acid concentration for His and Phe were made around pH 6, to avoid any carbonate interference and to allow the structure of the amino acid complex to be more closely defined. In the absence of CO_2, addition of excess Phe or His at pH 9 gave a relaxivity value of 2.3 mM^{-1} s^{-1} (20 MHz, 298 K), typical of a $q = 0$ complex with only an outer-sphere contribution. Addition of Phe and His to $[GdL^1(H_2O)_2]$ (1 mM, pH 6) over the range 0−150 mM gave rise to an incremental decrease in relaxivity that revealed a limit at 4.1 and 4.3 mM^{-1} s^{-1}, respectively, with an apparent binding affinity of 340(±40) and 260(±30) M^{-1}, respectively.

(31) The relaxivity of the triflate salt of $[GdL^1(H_2O)_2]^{3+}$ at 20 MHz and 298 K is partially limited by the relatively long τ_m value; examples of related diaqua complexes of comparable molecular volume (and hence τ_r) with relaxivities of 10.0 and 12.3 mM^{-1} s^{-1} have been reported: Aime, S.; Botta, M.; Fedeli, F.; Gianolio, E.; Terreno. E.; Anelli, P. *Chem. Eur. J.* **2001**, *7*, 5262; Messeri, D.; Botta, M.; Lowe, M. P.; Parker, D. *Chem. Commun.* **2001**, 2742.

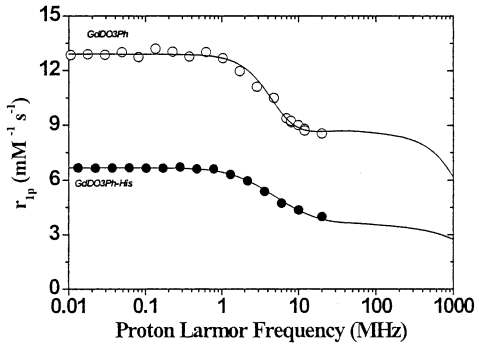

Figure 11. NMRD profile for $[GdL^1]^{3+}$ (20 MHz, 298 K, pH 6.2) showing the experimental data in the absence (open circles) and presence (filled circles) of excess added His. The lines show the best fit of the experimental data to the relaxation parameters, e.g. for the His adduct: $\tau_r = 140$ ps, $q = 1$, $\tau_m = 7$ μs, $\tau_v = 6.6$ ps.

The limiting relaxivity values are in the range expected for a $q = 1$ complex, in the absence of any large second sphere contribution.[2,3] Note that these association constants were recorded at a different pH than those of the Eu analogues discussed above.

The NMRD profile for the adduct with His was examined (Figure 11) and could be fitted very well by assuming that τ_m increased from 1.5 μs in the diaqua species[6] to 7 μs in the His adduct, accompanied by small increase in τ_r from 120 to 140 ps. This slowing of the water exchange rate at Gd in the His adduct is in contrast to the observations made with the phosphate or fluoride complexes, where the exchange rate increased by a factor of 10.[6] Independent verification of the change in water exchange rate was provided by examining VT ^{17}O NMR measurements. Data were collected at 2.1 T in the presence of a 25-fold excess of His using 20% ^{17}O-enriched H_2O. The observed transverse relaxation rate (R_2) vs T profile was fitted to the Swift−Connick equations[32] using standard procedures and gave $\tau_m = 8$ μs [$\Delta H_m = 75(\pm 3)$ kJ mol^{-1}] and $\tau_v = 6.6$ ps. The similarity in the τ_m value obtained lends support to the value obtained by independent NMRD analysis. An explanation for the slowing of the water exchange rate is provided by the role of the proximate protonated amino group. This may serve as a strong H-bond donor to a second sphere water molecule which, in turn, may act as a H-bond acceptor to the Gd-bound water (Scheme 1). The stability of this hydrogen-bonded array may enhance the activation energy barrier for the dissociative water interchange process and hence slow the rate of water exchange. This structure may also be regarded as an intermediate in the formation of the N,O-chelated adduct, as the acid concentration falls.

Preliminary Examination of Protein/Peptide Binding

Binding of $[GdL^1(H_2O)_2]^{3+}$ to human serum albumin (HSA) was examined by VT ^{17}O NMR and by the variation of the proton relaxivity with protein concentration. R_2, in the presence of 1.8 mM HSA, showed less than a 20% change ($R_2 = 10$ s^{-1}; 4.5 mM [GdL]; 1.8 mM HSA, 2.1 T, pH 6.2) over the temperature range 278−325 K, consistent with the behavior of a $q = 0$ ternary complex. Prior work with [GdDO3A] and its *N*-benzyl analogues had revealed similar behavior, and the corresponding Eu analogues were shown to be $q = 0$ complexes

(32) Swift, T. J.; Connick, R. E. *J. Chem. Phys.* **1962**, *37*, 307; Aime, S.; Botta, M.; Fasano, M.; Paoletti, S.; Terreno, E. *Chem. Eur. J.* **1997**, *3*, 1499.

Table 6. Crystal Data

compound	[YbL^1-acetate]	[YbL^1-glycinate]	[YbL^1-serinate]	[EuL^1-citrate]
empirical formula	$[C_{40}H_{56}N_7O_5Yb]^{2+}(CF_3SO_3^-)_2\cdot 3H_2O$	$[C_{40}H_{57}N_8O_5Yb]^{2}(CF_3SO_3^-)_2\cdot 2H_2O\cdot MeOH$	$[C_{40}H_{57}N_8O_5Yb]^{2+}(CF_3SO_3^-)_2\cdot 2H_2O\cdot MeOH$	$[C_{44}H_{58}N_7O_{10}Eu]\cdot 11H_2O$
formula weight	1240.15	1269.19	1298.21	1195.11
T (K)	120	120	120	100
crystal system	monoclinic	triclinic	triclinic	monoclinic
space group	$P2$ (no. 4)	$P1$ (no. 1)	$P1$ (no. 1)	$P2_1$ (no. 4)
a (Å)	12.277(4)	11.392(2)	11.288(2)	11.426(2)
b (Å)	16.040(4)	11.591(2)	11.981(2)	19.727(3)
c (Å)	13.277(4)	12.421(2)	12.454(2)	11.903(2)
α (deg)	90	64.30(1)	64.70(1)	90
β (deg)	102.20(2)	78.19(1)	76.53(1)	93.776(4)
γ (deg)	90	63.07(1)	62.42(1)	90
V (Å^3)	2546(1)	1317.6(4)	1348.4(4)	2677.0(7)
Z	2	1	1	2
$\Theta_{min}/\Theta_{max}$	2.02/29.00	2.01/39.46	2.04/39.00	1.71/27.50
data collected	31329	39412	29245	28099
data unique	13273	27144	25522	12191
data obsd, $I > 2\sigma(I)$	12849	27134	25516	11102
parameters	681	715	719	754
restraints	46	3	3	0
F_{000}	1262	647	662	1248
largest peak/hole	0.904/−1.064	2.126/−0.863	2.739/−1.027	0.642/−0.639
absorption correction	integration	integration	integration	multiscan
T_{min}/T_{max}	0.566/0.767	0.571/0.729	0.483/0.735	0.851/1
wR_2	0.057	0.050	0.063	0.071
R [$I > 2\sigma(I)$]	0.023	0.023	0.025	0.030
Flack parameter	−0.005(4)	−0.014(2)	−0.015(3)	−0.015(6)

Scheme 1

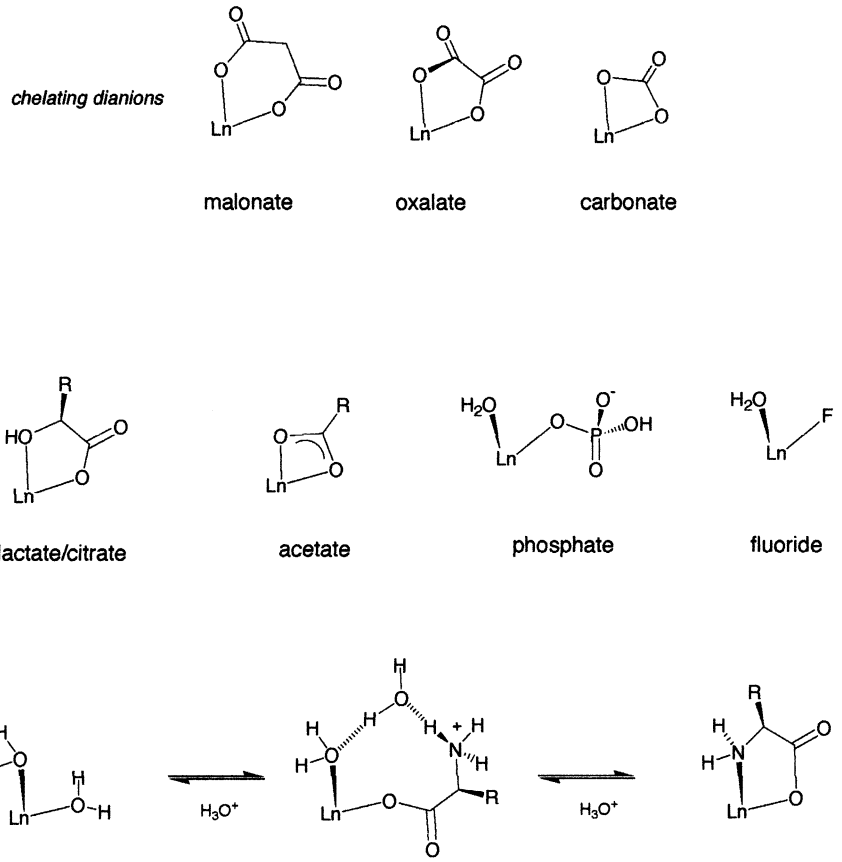

in the protein-bound complex by examination of luminescence lifetime measurements in water and deuterium oxide.[33] The change in relaxivity with added protein was fitted to a two-site model, giving $K_a = 1.5 \times 10^5$ M^{-1} and a limiting relaxivity of 21.8 mM^{-1} s^{-1}.[33] The high limiting relaxivity for this $q = 0$ adduct reflects the large contribution of second sphere waters and of labile protein protons in the vicinity of the Gd ion. A similarly high value has been observed for the more weakly bound $q = 0$ complex involving [GdDOTP]$^{5-}$ and HSA.[34]

(33) Aime, S.; Botta, M.; Fasano, M.; Geninatti Crich, S.; Terreno, E. *J. Biol. Inorg. Chem.* **1996**, *1*, 312.

(34) Aime, S.; Gianolio, S.; Terreno, E.; Pagliarin, R.; Giovenzana, G. B.; Lowe, M. P.; Sisti, M.; Palmisano G.; Botta, M. *J. Biol. Inorg. Chem.* **2000**, *5*, 488−497.

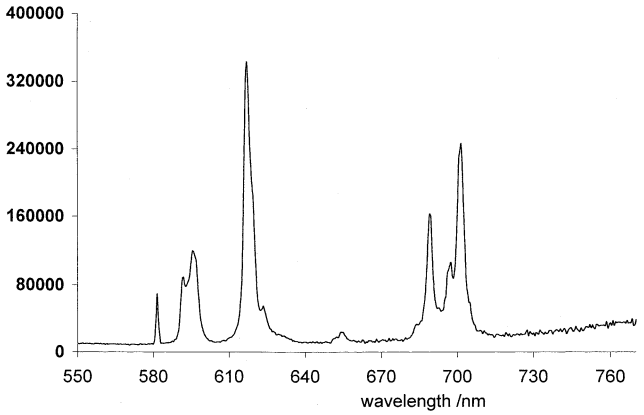

Figure 12. Emission spectrum of $[EuL^1]^{3+}$ in the presence of Gly-Asn (295 K, pH 7.4, 0.1 M MOPS buffer).

Emission spectra of the adducts of $[EuL^1]^{3+}$ with Gly-Ala, Gly-Asp, and Gly-Asn were recorded in the presence of excess added peptide (295 K, pH 7.4, 0.1 M MOPS buffer) and were compared to those obtained with serum albumin (1.8 mM), Glu-Ala-Glu, and Asp-Ser-Asp-Pro-Arg. The emission and CPL spectra were very similar in each case with a separation between $\Delta J = 1$ components of 3.5 nm and a more intense $\Delta J = 0$ band than had been observed with Ser, Phe, or His alone (Figure 12). Indeed, the spectra resembled that obtained with excess sodium acetate (0.3 M; 1 mM complex), suggesting a common chelated carboxylate structure involving either a Glu or Asp side chain or a C-terminal amino acid. However, a more detailed study of the interaction with the analogue $[YbL^1]^{3+}$ is merited, as the ^{1}H NMR dipolar shift of the axial ring proton is a more sensitive probe of the Ln coordination environment and parallel CD and CPL studies might also provide additional useful information to map the preferred complex binding site. In this respect, the enhanced shifting ability of the $[TmL^1]^{3+}$ analogue also offers considerable scope, in the pursuit of a selective NMR probe to aid protein structural analysis.

Conclusions

The structures of the ternary adducts of a series of oxyanions and amino acids with coordinatively unsaturated, chiral lanthanide complexes have been defined. Chelating dianions act as bidentate ligands, reversibly forming $q = 0$ complexes in aqueous solution, while mono α-OH- and α-amino carboxylates also form a chelated structure with no bound water molecules (Scheme 1). In more acidic media, amino acids form a $q = 1$ complex with a strongly hydrogen-bonded network that slows down the rate of water exchange at the Ln center. Fluoride and hydrogen phosphate are monodentate donors giving $q = 1$ species. Across the Ln series, affinity follows the variation in charge density, in the absence of any steric inhibition.

The polarizability of the axial donor plays the dominant role in determining the magnetic anisotropy factor that defines the spectral form and dipolar NMR shift of these monocapped square antiprismatic Eu and Yb complexes.

Experimental Section

Details of the methods and instrumentation used for NMR, relaxometry, and Eu luminescence emission studies are given in refs 6, 11, and 12.

Yb Luminescence Measurements. The kinetic behavior of the near-IR luminescence from ytterbium complexes was determined using a spectrometer built in-house. The samples were pumped using the fourth harmonic of a Q-switched Nd:YAG (Spectra Physics DCR-11) which produced a 10 Hz train of 266 nm pulses, with a typical duration of 8 ns fwhm and an energy of 0.1−1.0 mJ per pulse. The luminescence was collected at 90° to the excitation pulse and a monochromator (Jobin-Yvon Triax 320) used to select the desired wavelength, which was detected by a liquid nitrogen cooled germanium photodiode/amplifier (North Coast EO-817P) operating in high sensitivity mode. Under these conditions the detector has a rise time of ca. 200 ns and a fwhm response of 400 ns. The signal was captured and an average of 16 shots was recorded by a digital storage oscilloscope (Tektronix TDS320) and transferred to a PC for analysis. Instrument response functions were obtained using the fluorescence from a solution of a red laser dye (DCM), $\tau_F = 2.2$ ns. The lifetime of this dye is very short compared to the response time of the detector and therefore can be considered to provide an instrument response profile for the detection system and is used as an alternative to a scatterer.

Data Analysis. The luminescence lifetimes from ytterbium complexes are comparable with the detector response time, and hence, the data for the complexes were analyzed by iterative reconvolution of the instrument response function with a single or double exponential decay, the best fit being judged by nonlinear least-squares analysis using Microsoft Excel. The details of this approach have been discussed elsewhere.[35]

$[YbL^1(H_2O)_2](CF_3SO_3)_3$. 1,4,7-Tris[(*R*)-1-(1-phenyl)ethylcarbamoylmethyl]-1,4,7,10-tetraazacyclododecane[6] (L^1) (100 mg, 0.15 mmol) was heated to reflux with ytterbium triflate (91 mg, 0.15 mmol) in dry acetonitrile (4 cm^3) for 18 h. The reaction solution was allowed to cool and was dropped onto stirring diethyl ether (40 cm^3), and the resulting white precipitate was collected by centrifugation and filtration. The solid was redissolved in the minimum of acetonitrile and the precipitation procedure repeated twice more. A white powdery solid resulted (56 mg, 46%): mp 160°; ν_{max} (KBr)/cm^{-1} 3264 (br, NH), 1623 (C=O); *m*/*z* (ES$^+$) 414 (100, M^{2+}); δ_H (200 MHz; D_2O). Partial assignment: 110 (1H, H_{ax}), 79 (1H, H_{ax}), 64 (1H, H_{ax}), 49 (1H, H_{ax}), 46 (1H H_{eq}), 31 (1H, H_{eq}), 27 (1H, H_{eq}), 23 (1H, H'_{eq}); −8 (9H, C-Me); −14, −17, −22, −23, −33, −36, −38, −47, −48, −72 (10H, H'_{ax}, CH_2-CO), −83 (1H, ring −NH).

Crystals of the complexes of $[YbL^1]^{3+}$ with acetate, lactate, glycinate, and serinate, suitable for X-ray analysis, were obtained from aqueous media (for Gly and Ser in 10% MeOH/H_2O) containing 10 mM complex and 100 mM anion. Single-crystal X-ray diffraction experiments were carried out using SMART CCD area detectors and graphite-monochromated Mo Kα radiation. The structures were solved by direct methods and refined against F^2 of all data, using SHELXTL programs.[36] Absolute configurations were determined from anomalous dispersion by the Flack method.[37] A summary of cell and refinement data is given in Table 6. The [YbL^1-glycinate] and [YbL^1-serinate] crystals are pseudo-isomorphous. Details of the structures with lactate have been reported in a preliminary communication.[12] Each of the ternary complexes gave positive ion ESMS spectra corresponding to the expected mass.

Acknowledgment. We thank EPSRC, MURST, and the Royal Society (R.S.D.) for support; this work was carried out under the auspices of the EC-COST Action D-18.

Supporting Information Available: Crystallographic files (CIF) as detailed in the text. This material is available free of charge via the Internet at http://pubs.acs.org.

JA020836X

(35) Beeby, A.; Faulkner, S. *Chem. Phys. Lett*. **1997**, *266*, 116.
(36) SHELXTL version 6.12; Bruker AXS: Madison, WI, 2001.
(37) Flack, H. D. *Acta Crystallogr*. **1983**, *A39*, 876.